

# Rapid prototyping for non-developable discrete and semi-discrete surfaces with an overconstrained mobility

Rupert MALECZEK\*, Kiumars SHARIFMOGHADDAM<sup>a</sup>, Georg NAWRATIL<sup>a</sup>

\* i.sd | Department of Design | University of Innsbruck  
Rupert.maleczek@uibk.ac.at

<sup>a</sup> Institute of Discrete Mathematics and Geometry & Center for Geometry and Computational Design,  
TU Wien

## Abstract

In recent years, technical folding, also known as structural origami, has been developed and implemented in many fields and applications to a wide range of materials. As many techniques are inspired by computational origami, their output is in most cases a three-dimensional mesh that can be developed without stretching or tearing in a planar mesh that represents a planar sheet of material. This is not only helpful in the fabrication of large spatial structures, but also in the design and development phase where the models can easily be built from planar sheets of paper. For geometries that cannot be folded from a single sheet, an assembly strategy is needed that allows for a high accuracy of the final model. We present a solution for the model making in the design phase, that uses 3D printing of a hinge that can be assembled with a simple snapping mechanism to facilitate the model making process. Based on the special class of T-hedral surfaces, the authors will show examples and methods for discrete and semi-discrete models with an overconstrained mobility. Therefore, the strategy will be shown and explained for straight- and curved foldlines, respectively. Although STL printers are becoming more popular, the focus lies on FDM printers as they are currently more commonly used in design and engineering offices, as well as by design- and architectural students.

**Keywords:** structural origami, technical folding, rapid prototyping, fabrication, transformable design, flexible quad-mesh, semi-discrete surfaces

## 1. Introduction

Fabrication from a sheet of material has many applications in a wide variety of fields. Although folding seems to be a simple process, the geometric, physical and structural constraints make it a complex, but interesting strategy for industrial applications. Current developments show that the advantages of such structures are widespread, not only in structural behavior, but also in their fabrication methods. Fabricating from sheet material in flat state allows for cheap, fast and precise prefabrication. Folding from a flat state into a three-dimensional one is another advantageous aspect.

For this reason, many research groups related to the building industry work on surface discretizations or optimizations for double curved surfaces in order to fabricate them from flat material (in bent or flat state) [1]. There are also attempts to use origami inspired methods for the generation and fabrication of deployable structures [2]. Here the research focuses on foldable configurations that can either be fabricated from a flat sheet of material, or in some cases, from two layers of material connected with hinges [3]. The use of structures that can neither be flat folded nor be fully developed, but have 1DOF (Degree Of Freedom) is very rare. The reasons can be manifold, but the authors think this is related to the fact that they are not trivial to design and fabricate.

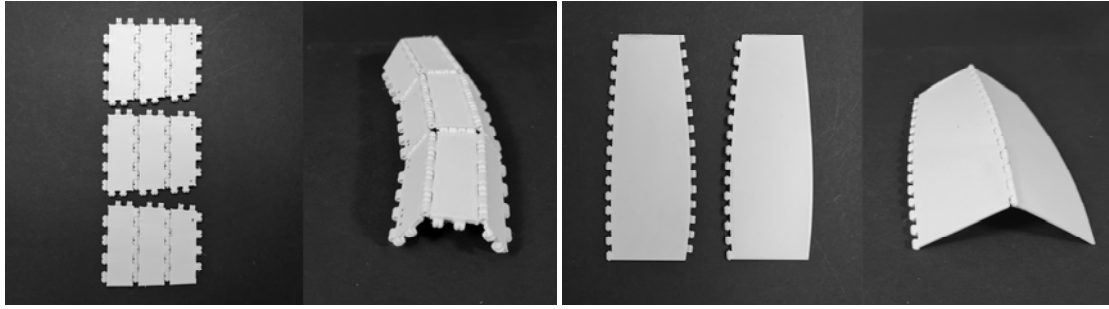


Figure 1: A discrete (left) and semi-discrete (right) example of the proposed hinge in printed and assembled state.

There is an ongoing investigation on discrete and semi-discrete T-hedral surfaces [4] [5] consisting of planar quads (PQ) and developable strips (D-strips), respectively, that involves mathematicians as well as architects and its related fields. As one aim of this research is the review of these surfaces for a potential architectural application, the question of model making popped up quickly. The standard approach with paper and scotch-tape, came to its limits as the accuracy question arose. As paper has a “weak” behavior during motion, especially when working with PQ-meshes, the authors needed to change the material. One could argue, that it would be easier to replace paper by cardboard, but that change will still not solve the scotched hinges. Even experienced model makers face difficulties in the assembly process and there will always be minor deviations along the foldlines. For these reasons, the authors decided to investigate 3D printed hinges from PLA (PolyLactic Acid), as it could solve the above described problematics: Generation of rigid or bendable parts with applied hinges, that allow for a high accuracy in the physical model, while the individual parts can be fabricated in flat state.

After introducing T-hedral surfaces and their constraints, the paper will present their 3D printed models, and the approach chosen for this particular solution. It will finally show and explain the 3D printed hinges on PQ-meshes as well as on semi-discrete meshes that bend during assembly and motion.

## 2. T-hedral Surfaces

A T-hedron can be seen as a generalization of a discrete surface of revolution in such a way that the axis of rotation is not fixed at one point but traces the so-called *prism polyline* on the base plane, which is orthogonal to the axis direction. Moreover, the action does not need to be a pure rotation but can be combined with an axial dilatation. After applying these transformations to the vertices of the *profile polyline*, a quad-surface with planar trapezoidal faces is obtained. The polygonal path of the profile vertex located in the base plane is called *trajectory polyline*. Therefore, the complete geometric information of the T-hedron is encoded within three polylines (Fig. 2b).

If only the profile polyline is replaced by a smooth profile curve, we end up with a so-called semi-discrete T-surface of the *vertical kind* (Fig. 2a). If the trajectory and prism polylines are replaced by their smooth analogues (i.e. trajectory and prism curve) the discrete kinematic generation of the surface gets continuous and we end up with a semi-discrete T-surface of the *horizontal kind* (Fig. 2c).

It can easily be seen [1] that the smooth strips of semi-discrete T-surfaces are developable (D-strips), making them interesting for practical applications. Note that only for special choices of the input polylines/curves, one can obtain T-hedral surfaces which are on the whole developable and/or have the flat-foldability property; e.g. the Miura-ori pattern (developable and flat-foldable) or the eggbox pattern (non-developable but flat-foldable).

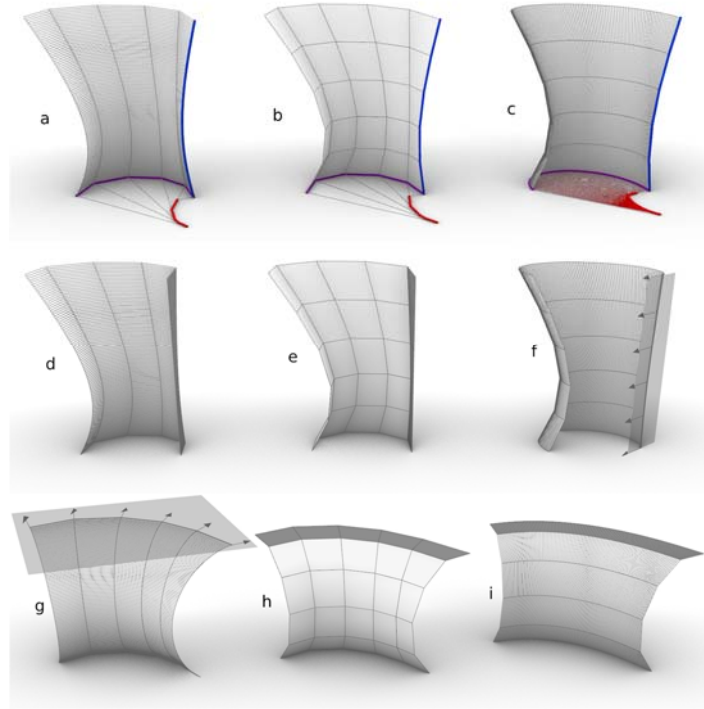


Figure 2: Discrete (b) and semi-discrete (a,c) T-surfaces constructed by profile (blue), trajectory (purple) and prism (red) curves/polylines in their initial states (deformation factor  $s = 1$ ). The vertical flexion limits ( $s < 1$ ) and horizontal ones ( $s > 1$ ) are illustrated in (d,e,f) and (g,h,i): Planar strips/tangent planes are shown in dark/transparent gray.

### 2.1 Isometric deformations and their limits

According to [6], each T-hedon allows a 1-parametric rigid-foldability, which is not self-evident as a PQ-mesh is in general rigid. Therefore, the T-hedral mobility is even overconstrained. Similar statements hold for the semi-discrete cases for which we refer to [5].

According to [6], the flexion limits of a T-hedron are reached as soon as either a PQ-row (Fig. 2h) or PQ-column (Fig. 2e) gets completely flat. The flexion limits for the semi-discrete T-surfaces can be argued from those of the discrete case on the one hand and from those of the smooth case on the other hand, which is discussed in detail in [7]. Thus, for the semi-discrete version of the vertical kind, the flexion limits are reached if either a D-strip gets completely flat (Fig. 2d) or a D-strip has a ruling with a horizontal tangent plane (Fig. 2g). For the horizontal kind, the flexion limits are reached if either a D-strip gets completely flat (Fig. 2i) or a D-strip has a ruling whose tangent plane touches along the entire associated profile polyline of the semi-discrete surface (Fig. 2f).

If a complete PQ-strip of a T-hedron or a D-strip of the semi-discrete T-surface gets flat, then the structure is also in a so-called bifurcation configuration, as it can transition from one working mode to another. As this transition configuration is, at the same time, a flexion limit, the T-hedral surface can only flex back, but the PQ-strip/D-strip can flip to opposite sides (Fig. 3).

### 3. Model Making

In the design phase, models are always helpful in order to create a better understanding of certain geometries. Been said, for foldable geometries, this is a crucial process, as the model can be investigated not only visually, but also haptically. For this reason, model making is also a classical teaching and investigation method, introduced already in the era of the Bauhaus [8].

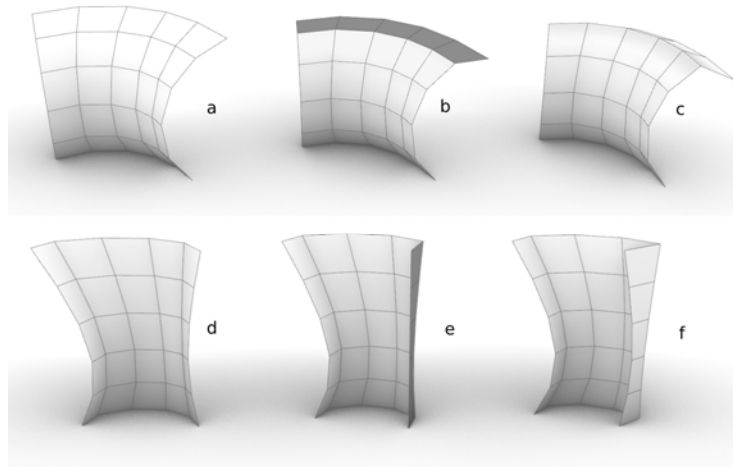


Figure 3: A T-hedron in horizontal (b) and vertical (e) bifurcation configurations (= horizontal and vertical flexion limits). The two possible states for the top PQ-column PQ-row and right, which belong to different modes, are illustrated in (a,c and d,f) respectively.

In the context of technical applications, making a physical model is sometimes the most important part of the work, after generating a foldable digital one. It is sometimes even the driver of innovation, as some geometries that were made foldable through computation underlined the proof by the model itself [9]. As interesting as paper models are for some investigations, sometimes they behave in a not obviously predictable way. Thus, some of them might not exist in a pure geometric matter [10].

Folding models from paper or cardboard of a good quality, requires extensive experience. Even machine pre-creased sheets are challenging to form without unwanted wrinkles or other fabrication caused artifacts on the surface. For complex mechanisms, a high model quality is necessary, as small local deviations can change the motion behavior or even block the mobility of the entire system. In that case, the model would no longer support the investigation of the designer.

For geometries that are only patchwise developable, this process becomes even more delicate, as the process changes from pure folding to partial folding and assembling. The assembly might lead to stiff structures [11] [12] if the rotation along a foldline is blocked, or a deployable one if the foldline is articulated as a hinge [3]. If the model should still be made from paper or cardboard, scotch-tape as assembly and hinge solution can be a potential approach. The increasing complexity of the individual parts makes this approach less confident as the tape is sometimes applied under slight tension, and therefore causes unwanted pretension and bending in the model.

For this reason, the authors propose 3D printed parts, that can snap together, as a fast and accurate method in the model making process.

### 3.1 3D Printing and Folding

Folding and 3D printing have been related since the early days of 3D printing. Printer accuracy or “first” printed models are often parts in the form of an animal that have integrated hinges, so they are flexible after the printing process. From dinosaurs to horses, there is a wide variety of basic models, as well as more advanced models as e.g. bistable mechanisms to find [13]. The range of hinge-solutions for foldable models that can be printed flat is enormous. From compliant hinges, to more complex solutions as e.g. proposed by Suto [14], a wide range of standard solutions is available. As they require a fully developable mesh, they are not suitable for T-hedral surfaces.

For this investigation, the printable hinges have to fulfil several constraints: They should allow for a fast and accurate assembly, they should be printable without any complex support, that needs to be removed after the printing process, and they should allow as much rotation as possible, without an additional part.

Although there is a lot of development in the 3D printing industry and raising printers are becoming more affordable, the authors focus on FDM printers with PLA. As PLA can be shredded and recycled, it starts to become a circular material system. In addition, many students and companies already have small and cheap FDM printers in their homes/offices. Moreover, it seemed to be interesting to work with the most standardized nozzle diameter of 0.4mm. Therefore, all test prints were either made with a Prusa Mk3 or an Ender 5, as those two models represent widespread affordable consumer FDM printers. All tests and prints for this paper were made with the same PLA-Type [15].

### 3.2 Hinge Types

The number of hinges that can be 3D printed is manifold, and it would exceed the paper to mention all possible ones here. Therefore, the authors will focus on hinges that can be printed flat and allow an assembly in a non-flat as well as in a flat state.

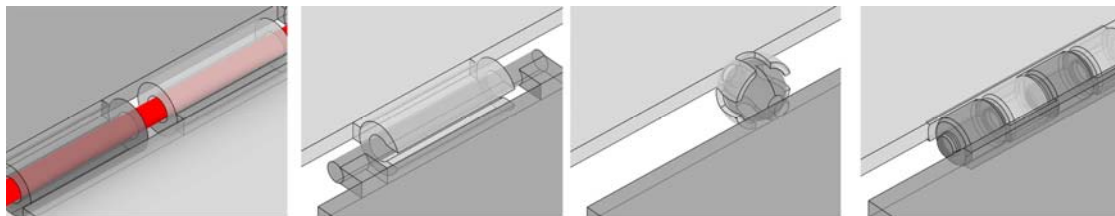


Figure 4: Hinge types from left to right: RH-String, RH-DSnap, SH-Snap, and RH-Snap.

At the beginning of the investigation, the authors were looking for existing solutions that could work for their particular use. Three existing types could be identified that would work for T-hedral surfaces. From these potential solutions, two were combined to generate a solution that can be printed and assembled in a short amount of time.

For discrete models, rotational hinges (RH) are a very convenient solution, as they allow only the rotation necessary for the mechanism. To assemble a RH, either an additional element that is placed in the center of the rotational axis (RH-String/Fig. 4a), or an element that allows for snapping in a certain direction is required (RH-DSnap/Fig. 4b).

For semi-discrete models, spherical hinges that snap (SH-Snap/Fig. 4c) are a good solution, but cause problems within the printing process. To keep the properties suitable for discrete and semi-discrete models, the authors developed a rotational hinge with a snapping pin (RH-Snap/Fig. 4d) that also allows a partly spherical rotation based on its design.

The rotational hinge with an internal string (RH-String) consists of alternating hollow tubes connected, with a continuous string (e.g. filament), in the rotational axis. It is potentially a good solution, but requires a lot of work guiding a string through the hollow cylinders. The assembly becomes very unlikely, when the geometry is complex, as the string requires a sliding direction. Printing hollow cylinders works properly and can be done with a relatively fast printing speed, if the cylinders' axes are parallel to the printing bed.

If the string is replaced by a small printed cylinder, the second cylinder needs to have an opening that allows it to snap the two elements together. This opening defines an assembly direction (RH-DSnap). These hinge types are potentially interesting solutions for models with not too complex starting geometries. One remaining danger is that the sliding direction of each part in a folding row must be different to its neighboring parts, so the entire model will not fall apart in a certain folding position. It

would require excessive calculation effort, to generate a proper model, which makes the intent of a low-threshold access difficult, especially for semi-discrete models.

As straight foldlines would be sufficiently solved with a RH, spherical-hinges (SH) are an interesting solution for semi-discrete models, as a linear axis connected to a plate will block some bending in this area. They consist of two parts that can be snapped together (SH-Snap). Printing them with an FDM printer in a small scale is a challenging task. The printed sphere is in a small scale, seldom perfectly round, as the first layer is either sticking to the printing bed or printed at a small distance from the printing bed. The counterpart of the sphere is even more difficult to print as it has some slits, and is therefore mostly printed in the air (without supports). Model series during the investigation have shown that this hinge starts to work properly, when the printed female parts of the hinges have a thickness of 4 times the nozzle diameter and the sphere has a diameter of 7mm. In relation to a thin plate that bends and a thin pin connector, this solution was not suitable for the authors.

As a solution that can work for discrete and semi-discrete models, the authors propose a R-hinge with a snapping pin solution (RH-Snap). Cylinders are relatively fast to print with a FDM printer, and allow for a smooth rotation of the hinge. If there is no particular sliding direction for the assembly itself, designers can focus on the geometry constraints instead of the hinge detailing. A cylindrical pin with a chamfered end also allows spherical motions and is therefore suitable for curved foldlines.

### 3.3 Snapping Pin Hinge

The RH-Snap is a variation of a classical cylindrical hinge, consisting of two parts, namely a cylinder with pin (male) and a hollow cylindrical tube (female). The two cylinders have identical outer radii ( $r_z$ ) and an identical length ( $l_z$ ) along one foldline as well as an identical chamfered edge defined by a length and height in relation to  $l_z$ . The radius of the pin ( $r_p$ ) is slightly smaller than the radius of the hole ( $r_h$ ) in the hollow tube. The pin's end is chamfered and the inner wall of the hole has a spherical end part, allowing for better assembly and additional spherical DOFs. The pin's length ( $l_p$ ) is also defined by the overlapping of the different elements.

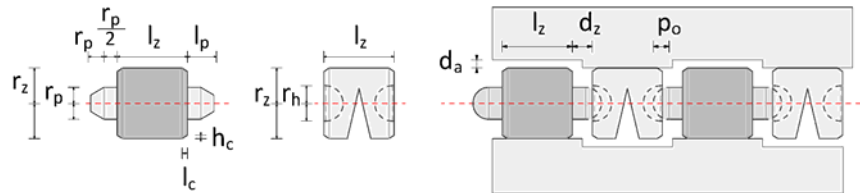


Figure 5: Description of the male- and female part with optional slit, that form a RH-Snap (left) and its assembled state (right).

The printing tests have shown that the smallest working pin-radius  $r_p$  is 0.9 mm and the associated  $r_z$  is therefore 2mm. For a better assembly and bending behaviour, a V-shaped slit can be implemented to allow the female parts a certain deformation.

The length of the pin  $l_p$  is defined by the distance  $d_z$  and the pin-overlap  $p_o$ . As  $p_o$  has an influence on the assembly, as well as the resistance before the disassembly of the parts, these values need to be considered in relation to the printers available. For the standard printers,  $p_o$  was chosen with 0.3mm and  $d_z$  with 0.4mm. The chamfer on the pin and the female part edges allow the pin to snap inside.

As the printing process might be relatively rough, the air gap between the pin and the hole needs to be large enough to allow rotation, but small enough so that the pin will not pop out if bent too much. Therefore,  $r_h$  is  $r_p$  plus 0.2mm (equals half nozzle diameter).



Figure 6: Detail of the still working RH-Snap element and a semi-assembled curved foldline.

The cylinders' lengths are calculated by the length of the foldline that needs to be assembled. The minimum length of  $l_z$  is 3.6mm. If calculated for a foldline,  $d_z$  needs to be added, so 4mm is a good value for this calculation. If we consider four cylinders, then 16mm should be the shortest foldline in the entire folding system.

As the cylinders should be fixed to the plates along the entire length  $l_z$  it is evident that discrete and semi-discrete models require different approaches for  $l_z$  (see Section 4). For a nice motion, there should be an air-gap  $d_a$  to the neighboring plate, with a minimum of 0.25mm.

## 4. Results and Discussion

If a geometric model needs to be printed, not only the hinge-design is important, but also the plate design of the faces. Additionally to the snapping pin hinge, the plate design influences the entire behavior of the physical model. In the beginning, the authors were experimenting with the plate thickness in relation to the cylindrical elements of the hinge. From a printing perspective, a plate thickness identical to the outer cylindrical diameter would be advantageous, as no support structure needs to be printed, and the lower part of the plate would have a nice and clean texture. The problem might then be the bending behavior of the plate, that is reduced as the plate's stiffness is related to the thickness. If the plate thickness is smaller than the cylinder's diameter, an eccentric positioning of the plate might cause problems in the motion behavior linked to the rotation limit in the axis of rotation. As the authors wanted to investigate entire mechanisms with the least possible restrictions, the plate is always located in the zero thickness plane of the geometric model. However, the eccentric solution can still be interesting for other purposes or applications.

### 4.1 Models of T-hedra

Initially, the investigation started with discrete models. The focus was on a reduced design of the panels and the hinges. Printing thin plates, not directly on the printer's bed, causes some problems, mainly the loss of printing speed, as the material needs to have some construction under it, or cantilever for a long distance. Printing with a thin raft, helps cheap printers to gain a good and fast print. For the plate stiffness, 6 to 8 layers of material are sufficient to make stiff enough plates for rigid panels. As described above, four cylinders per foldline are enough to have a smooth rotation of the elements. Of course, other panel-designs such as simple X-frames or other patterns are interesting, but this discussion would exceed the frame of this paper.

What is important in the investigation of the discrete models is the rotation limit of the plates themselves. For the thinnest rigid plates, a rotation limit of 65 degrees can be achieved. If a folding angle beyond that one is necessary, additional elements need to be implemented that complicate the snapping assembly process. Therefore, these elements are not topic of this paper.

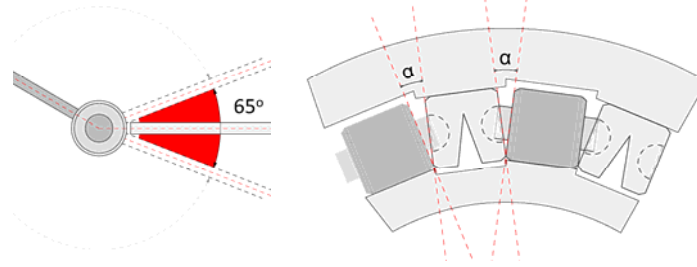


Figure 7: Rotation limits of the RH-Snap (left) and its conical limits ( $\alpha = 12^\circ \pm$  printing inaccuracy) of the additional spherical DOFs (right).

For the fabrication of T-hedra, not only the individual panels can be unrolled and printed, but entire unrolled patches can be printed. All preparations of the models are done in 2D based on the unrolled meshes, whereas the mesh-edges will become the cylinders' axes of rotation. As the plates need to be snapped together, the assembly will self-adjust to one proper spatial state.

Similar to the semi-discrete models, the patches can be generated as PQ-columns or PQ-rows (see Fig. 8). The snapping pin hinges can also be printed in an assembled state, for a faster assembly.

As the offset of the plates is done in both directions, the mechanism might get difficulties known from thick folding [16] [17]. To avoid these problems that occur in our case in degree four vertices, the authors would advice to avoid hinges close to the vertices. Therefore, a distance of 2mm from vertices should be respected.

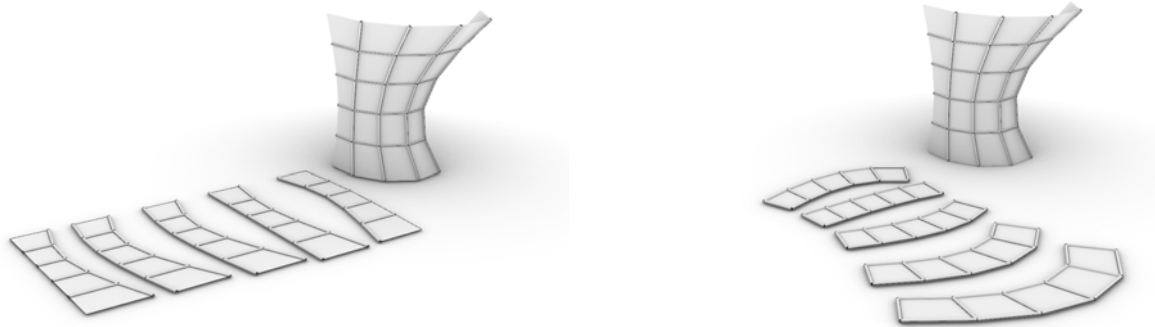


Figure 8: A T-hedron with developable PQ-columns (left) and PQ-rows (right), respectively.

#### 4.2 Models of Semi-Discrete T-surfaces

Semi-discrete T-hedral surfaces require a different approach for fabrication. As the foldlines and the panels change from straight to curved, bending starts to play a role. As the model changes from straight-to curved folding, a different approach in the consideration for the hinge distribution and the plates is required.

Instead of rigid panels, bendable ones are needed. For this reason, the offset can be reduced to four times the layer thickness. If the plates have a constant thickness, they will bend with a constant distribution of the bending energy only stressed in the desired direction by the hinges.

If the hinges are distributed based on the shortest possible length of the cylinder, the number of hinges can vary along each foldline. If the maximum curvature is modest, this strategy is sufficient. However, as explained by Tachi [16], rulings allow for a good control of the behavior of curved folded surfaces. As the rulings should be located between two hinges, the number of hinges is identical on all foldlines in one model, but differ in the length  $l_z$ . For this reason, the shortest foldline of a semi-discrete model is

used to define the number of hinges in the entire system. Moreover, the rulings along the whole semi-discrete surface can easily be generated based on the discretization of the shortest foldlines implied by the lengths of the hinges. As for the semi-discrete T-hedral surfaces of the vertical kind, the rulings are parallel to the base plane (D-strips are parts of cylinders), they can easily be incorporated into the 2D printing model. For the horizontal kind, the D-strips are, in general, parts of tangent surfaces of space curves. Thus, they have to be developed together with the panel, which is a little bit more cumbersome.

As the plate thickness should be reduced for better bending behavior, a triangle-shaped slit is generated along the rulings. In that way, the printed plate consists of only three layers, covering the tip of this triangle. Usually, the ruling-based slits in the material would be in the compression zone of the material, but in this small scale, this seems not to have a significant influence on the model, as it will not break as e.g. wood [18].

As shown in Fig. 7 the hinge's connection allows for some rotation outside the foldline's tangent. This spherical motion becomes critical when two neighboring cylinders touch each other, and start to change the centre of rotation to this touching point. In the investigated case, the angle between two cylinders should be below  $12^\circ$ . However, it has been said that the printing process can produce inaccuracies that can make this angle larger or smaller. Above this angle, the foldline's hinges will add some bending stiffness to the entire model. This and the effects of the choice of semi-discretization (horizontal or vertical) on the bending behavior of a geometric shape are discussed in Section 4.2.1.

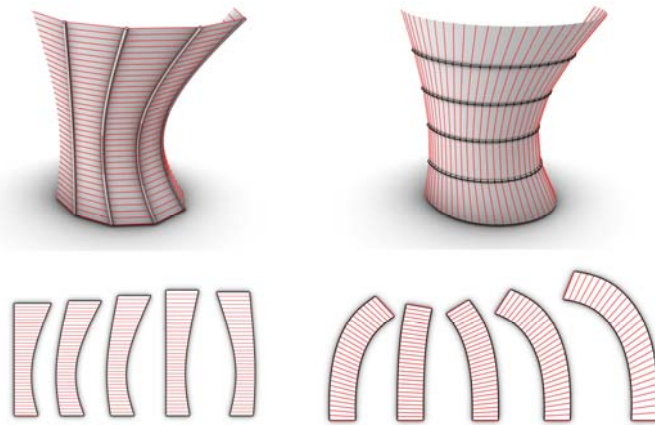


Figure 9: A semi-discrete T-surface with its developable strips in columns- (left) and row (right) direction.

The decision if the surface has horizontal or vertical D-strips, can be design or fabrication driven. This decision can either be based on a design idea, or on other constraints such as available sheet size or 3D printing volume of the available printer.

#### 4.2.1. Evaluation of the Bending Energy in Semi-Discrete T-surfaces

In the design phase, it is advantageous to have a first real-time evaluation of the bending energy needed to flex the semi-discrete T-surface. For doing that, we use the following geometry-based approach.

It was shown by Ge et al. [19] that the energy stored in a surface  $S \in \mathbb{R}^3$  bent from an inextensible plate of area  $A$ , can be expressed in terms of the mean curvature  $H$  and Gaussian curvature  $K$  by

$$\int_S (4\mu + 2\lambda)H^2 - 2\mu K \, dA \quad (1)$$

where  $\lambda$  and  $\mu$  are the so-called Lamé constants. In our case,  $S$  is a developable surface which implies  $K = 0$  thus the bending energy of the surface is directly proportional to  $\int_S H^2 \, dA$ . We aim to compute the bending energy  $B$  in the D-strips of the semi-discrete T-surfaces based on a discretized approach, as

only for some special cases an analytic description of the smoothly bent strips under the T-hedral deformation is available [5]. Therefore, we discretize our D-strips into slim trapezoids, where the vertices are on the rims of the D-strips. As we are dealing with a developable surface, an edge-based discretized computation of  $B$  along the rulings  $e$  seems to be the most natural choice, which is directly proportional (depending on the material and thickness of the plate) to the expression

$$W = \sum_e |e|^2 A^{-1} \theta^2 \quad (2)$$

according to [20] [21] [22], where  $A$  is some area associated with  $e$ . In our case, we choose for  $A$  the mean area of the two trapezoids adjacent to  $e$ . Moreover,  $\theta$  denotes the exterior angle enclosed by these two trapezoids along  $e$ .

Due to the used bent plates, a semi-discrete T-surface is stressed and tends to deform into a local minimum of the bending energy function within the deformation interval, which can be bounded by (a) flexion limits (cf. Section 2.1), (b) self-collisions, (c) joint limits or (d) bending limits of the plates. During the T-hedral deformation  $W$  is monotonic, but the two kinds of semi-discretizations behave in an opposite manner (see Fig. 10). Thus, in theory, the semi-discrete T-surfaces always tend to deform to the limits of the deformation interval, which is also the preferred state for its assembling. The printed models (see Fig. 11) verify this theoretical result up to some minor deviations caused by irreversible plastic deformation of the plates during bending and friction in the hinges.

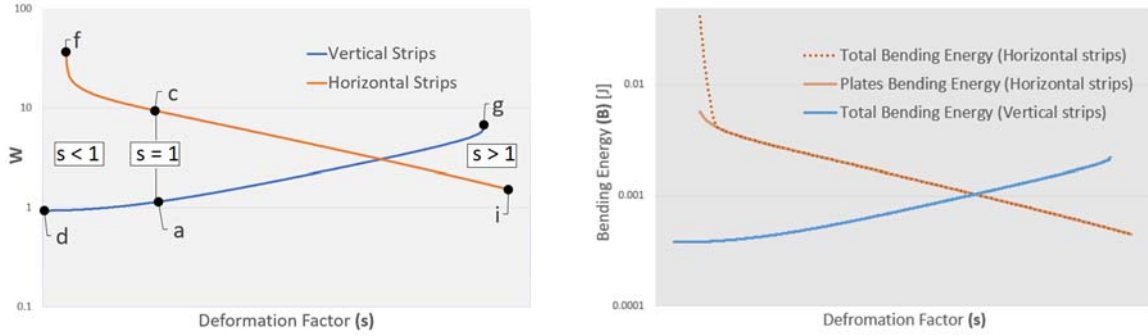


Figure 10: Bending energy evaluation graph for two different kinds of semi-discrete T-surfaces with vertical strips and horizontal strips. The graph of Eq. (2) on the left shows the connection to Figs. 2c,f,i and Figs. 2a,d,g. On the right the graphs of the bending energies  $B_{plate}$  and  $B_{plate} + B_{rod}$  of Eq. (3) and Eq. (4) are displayed. For the vertical strips no bending energy is implied by the hinges. According to [15] Young modulus  $E=3.12$  GPa is defined.

Moreover, there can also arise additional bending energy from the pin joint hinges (RH-Snap), if the angle  $\beta$  enclosed by the male and female parts of the hinge violates the joint limit  $\alpha$ , which is illustrated in Fig. 7. In this case, the evaluation of the bending energy can be refined as follows: First, we have to concretize Eq. (2) in terms of the plate thickness  $h$  (three layers for the ruling-based slit plates), which yields

$$B_{plate} = \sum_e \frac{1}{24} E h^3 |e|^2 A^{-1} \theta^2 \quad (3)$$

according to [22], where  $E$  denotes the Young modulus. The energy formula for the smooth bending of a circular rod given in Eq. (18.11) of [23] can also be adapted for the discrete case as follows

$$B_{rod} = \sum_V \frac{1}{8} E \pi r_p^4 b^{-1} (\beta - \alpha)^2 \quad (4)$$

where  $V$  are the centers of the spherical caps of those male parts where  $\beta > \alpha$  holds,  $r_p$  denotes the radius of the pin and  $b$  is the mean of the lengths of the line-segments adjacent to  $V$ .

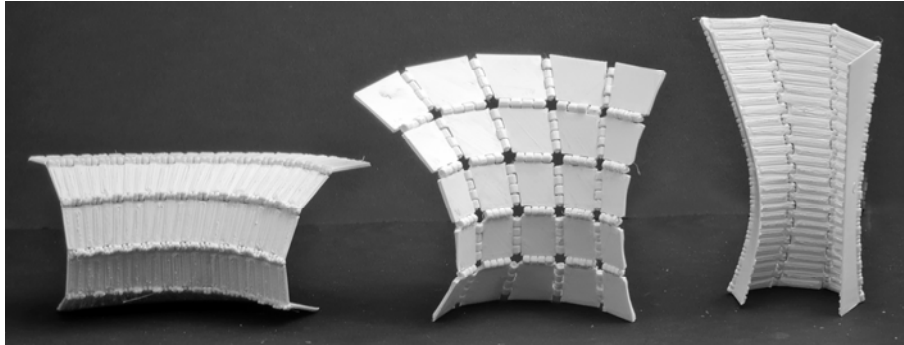


Figure 11: A PQ-mesh (middle) and its semi-discrete versions with horizontal D-strips (left) and vertical D-strips (right) based on the same reference surface corresponding to Fig. 2b, Fig. 2i and Fig. 2d respectively.

## 6. Conclusion and Outlook

Connecting two tailored sheets along a common edge is a classical problem in many fields. Connecting them with a hinge in order to be deployable, is a more complex problem. But if the advantages of such mechanisms should be applied to larger structures [3], then they are worth to be investigated. For this reason, this research can be seen as a pre-study for larger structures as the general question remains identical: Individual parts from sheet material connected with hinges to spatial deployable structures. As larger structures might not consist entirely of printable materials, the potential question might then be: What material the hinge be made from, if it is also a connection?

Moreover, it would also be interesting for practical applications to identify those semi-discrete T-surfaces where a slight change in the bending energy results in a significant variation of their spatial shapes; i.e. sensitive designs.

## Acknowledgements

The second and the third authors are supported by grant F77 (SFB “Advanced Computational Design”, subproject SP7) of the Austrian Science Fund FWF.

## References

- [1] H. Pottmann, A. Schiftner, P. Bo, H. Schmiedhofer, W. Wang, N. Baldassini and J. Wallner, „Freeform Surfaces from Single Curved Panels,“ *ACM Transactions on Graphics*, pp. 1-10, 2008.
- [2] T. Tachi, „Introduction to Structural Origami,“ *Journal of the International Association for Shell and Spatial Structures: J.IASS*, vol. 60, no. 1, 03 2019.
- [3] R. Maleczek, G. Stern, A. Metzler and C. Preisinger, „Large Scale Curved Folding Mechanisms,“ in *Impact: Design with all senses*, C. Gengnagel, O. Baverel, J. Burry, M. Ramsgaard Thomsen and S. Weinzier, Hrsg., Berlin, Springer, 2019, pp. 539-553.
- [4] K. Sharifmoghaddam, G. Nawratil, A. Rasoulzadeh and J. Tervooren, „Using Flexible Trapezoidal Quad-Surfaces for Transformable Design,“ in *Proceedings of the IASS Annual Symposium 2020/21 and the 7th International Conference on Spatial Structures*, 2021.
- [5] I. Izmetiev, A. Rasoulzadeh and T. J., „Isometric Deformations of Discrete and Smooth T-Surfaces,“ *in preparation*, 2022.

- [6] R. Sauer and H. Graf, „Über Flächenbiegung in Analogie zur Verknickung offener Facettenfläche,“ *Mathematische Annalen*, pp. 499-535, 1931.
- [7] R. Sauer, *Differenzgeometrie*, Springer, 1970.
- [8] D. Koschitz, „Designing with curved creases,“ in *Advances in Architectural Geometry 2016*, H. E. Z. vdf, Hrsg., Zurich, vdf, Hochschulverlag, AG, ETH Zürich, 2016, pp. 82-103.
- [9] T. Tachi, „Geometric Considerations for the Design of Rigid Origami Structures,“ in *IASS Symposium 2010 - Spatial Structures - Permanent and Temporary*, Shanghai, 2010.
- [10] E. D. M. Deimaine, V. Hart, N. Price and T. Tachi, „(Non)Existence of Pleated Folds: How Paper Folds Between Creases,“ *Graphs and Combinatorics*, vol. 27, no. 377, 2011.
- [11] H. Engel, *Tragsysteme*, Hatje Cantz Verlag, 1925.
- [12] J. Lienhard, *Bending-active structures : form-finding strategies using elastic deformation in static and kinetic systems and the structural potentials therein*, phd-thesis, Stuttgart, 2014.
- [13] Thingiverse.com, „<https://www.thingiverse.com/>“. 01 01 2018. [Online], [access on 15 06 2022].
- [14] K. Suto und K. Tanimichi, „Crane,“ Food4Rhino, 15 01 2022. [Online]. Available: <https://www.food4rhino.com/en/app/crane>. [access on 15 06 2022].
- [15] 3DJake.com, „3DJake.com,“ 08 08 2022. [Online]. [https://c-3d.niceshops.com/upload/file/Technical\\_Data\\_Sheet\[0\].pdf](https://c-3d.niceshops.com/upload/file/Technical_Data_Sheet[0].pdf). [access on 05 08 2022],
- [16] T. Tachi, „Rigid-Foldable Thick Origami,“ in *Origami 5*, Boca Raton, CRC Presse, 2011, pp. 253-264.
- [17] J. S. Ku und E. Demaine, „Folding Flat Crease Patterns With Thick Materials,“ *Journal of Mechanisms and Robotics*, vol. 8, no. 3, pp. 031003-1--6, 06 2016.
- [18] R. Maleczek, J. Mertens and V. Troi, „Double Curved Panel Forming with Bespoke Slits,“ in *ASME-IMECE Conference 2021*, Online, 2021.
- [19] Z. Ge, H. Kruse and J. Marsden, „The limits of Hamiltonian Structures in Three Dimensional Elasticity, Shells, and Rods,“ *Journal of Nonlinear Science*, vol. 6, pp. 19-57, 1996.
- [20] Z. Zorin, „Curvature-based energy for simulation and variational modeling,“ in *Proceedings of the International IEEE Conference on Shape Modeling and Applications*, 2005.
- [21] E. Grinspun, A. Hirani, M. Desbrun and P. Schröder, „Discrete Shells,“ in *Proceedings of the 2003 ACM SIGGRAPH/Eurographics symposium on Computer animation*, 2003.
- [22] L. Dudte, E. Vouga, T. Tachi and L. Mahadevan, „Programming curvature using origami tessellations,“ *Nature Materials*, 2016.
- [23] L. Landau und E. Lifshitz, *Theory of Elasticity*, Pergamon Press, 1970.